Inorg. Chem. **2003**, *42*, 6655–6666

Synthesis and Comprehensive Characterizations of New *cis*-RuL_2X_2 (X = Cl, CN, and NCS) Sensitizers for Nanocrystalline TiO_2 Solar Cell Using Bis-Phosphonated Bipyridine Ligands (L)

Hervé Zabri,[†] Isabelle Gillaizeau,[†,||] Carlo Alberto Bignozzi,*[,‡] Stefano Caramori,[‡] Marie-France Charlot,[§] Joan Cano-Boquera,*[,§] and Fabrice Odobel*[,†]

Laboratoire de Synthèse Organique, UMR 6513 CNRS, Faculté des Sciences et des Techniques de Nantes, BP 92208, 2, rue de la Houssinière, 44322 Nantes Cedex 03, France, Dipartimento di Chimica dell' Università di Ferrara, Centro di Studio su Fotorattività e Catalisi CNR, 44100 Ferrara, Italy, and Laboratoire de Chimie Inorganique, UMR 8613, Institut de Chimie Moléculaire et des Matériaux d'Orsay, Université de Paris-Sud, 91405 Orsay Cedex, France

Received April 16, 2003

The preparation and the properties of several ruthenium complexes of the general formula *cis*-RuL_2X_2 with L = 2,2′-bipyridine-4,4′-bisphosphonic acid, L′ = 2,2′-bipyridine-5,5′-bisphosphonic acid, and X = Cl, CN, or NCS are reported. The synthesis of these complexes relies on the preparation of the key intermediates *cis*-Ru(bipyridinebis-(diethyl ester phosphonate))Cl_2. The ground-state second pK_a values of the thiocyanato complexes were determined and are 6.0 and 6.1 for *cis*-$RuL_2(NCS)_2$ and for *cis*-$RuL'_2(NCS)_2$, respectively. For these species, ^{13}C NMR and IR demonstrate that the thiocyanato ligands are bound to Ru via the N atom. The new complexes exhibit a blue-shifted electronic absorption spectrum with respect to the analogous complexes containing carboxylic acid groups. Density functional theory molecular orbital calculations show that the LUMO of the bipyridine phosphonated ligands is at higher energy than the corresponding dicarboxylate complexes and that the thiocyanato ligands are not simple spectator ligands, whose role is to enrich electron density on the ruthenium, but are also involved in transitions from Π*Ru–NCS to Π*bpy that extend the absorbance of the dye in the low energy part of the absorption spectrum. The photoaction spectra recorded in a sandwich regenerative photovoltaic cell indicate that the cyano and thiocyanato complexes containing the bipyridine substituted in 4,4′ positions exhibit a 90–95% photoconversion efficiency on the MLCT band, whereas those containing the bipyridine substituted in 5,5′ positions display lower efficiency (60–65%). The most efficient complex in the series is *cis*-$RuL_2(NCS)_2$; however, its overall efficiency is about 30% lower than the analogue *cis*-$Ru(H_2dcb)_2(NCS)_2$ (H_2dcb = 2,2′-bipyridine-4,4′-dicarboxylic acid) due to a lower absorbance in the red part of the visible spectrum.

Introduction

Photovoltaic cells based on dye-sensitized wide-band-gap semiconductor electrodes have attracted much attention in the last years owing to the growing interest in solar energy conversion.[1] These types of solar devices contain a photoanode made of a dye sensitizer grafted on the surface of a nanocrystalline semiconductor electrode.[2] The most efficient sensitizers studied so far are based on ruthenium[2,3] or osmium[4] polypyridine complexes that are chemisorbed on the semiconductor surface via carboxylic acid groups. An alternative anchoring group is the phosphonic acid functionality which forms very stable bonds with most of the

* Authors to whom correspondence should be addressed. E-mail: fabrice.odobel@chimie.univ-nantes.fr,

[†] Faculté des Sciences et des Techniques de Nantes.

[‡] Università di Ferrara.

[§] Université de Paris-Sud.

[||] Institut de Chemie Organique et Analytique, UMR 6005 Université d'Orléans, rue de Chartres, BP 6759, 45067 Orléans cedex 2, France.

(1) (a) Dresselhaus, M. S.; Thomas, I. L. *Nature* **2001**, *414*, 332−337. (b) Turner, J. A. *Science* **1999**, *285*, 687−689.

(2) (a) Hagfeldt, A.; Grätzel, M. *Acc. Chem. Res.* **2000**, *33*, 269−277. (b) Hagfeldt, A.; Grätzel, M. *Chem. Rev.* **1995**, *95*, 49. (c) Kalyanasundaram, K.; Grätzel, M. *Coord. Chem. Rev.* **1998**, *77*, 347−414.

(3) (a) Nazeeruddin, M. K.; Kay, A.; Rodicio, I.; Humphry-Baker, R.; Mueller, E.; Liska, P.; Vlachopoulos, N.; Grätzel, M. *J. Am. Chem. Soc.* **1993**, *115*, 6382−6390. (b) Nazeeruddin, M. K.; Pechy, P.; Renouard, T.; Zakeeruddin, S. M.; Humphry-Baker, R.; Comte, P.; Liska, P.; Cevey, L.; Costa, E.; Shklover, V.; Spiccia, L.; Deacon, G. B.; Bignozzi, C. A.; Grätzel, M. *J. Am. Chem. Soc.* **2001**, *123*, 1613−1624.

10.1021/ic034403m CCC: $25.00
Published on Web 09/16/2003

transition metals and especially the hard Lewis acid metals such as Zr(IV), Ti(IV), or Sn(IV).[5]

The utilization of phosphonic acid groups for the immobilization of dyes on TiO_2 has been first reported by Grätzel et al.;[6,7] it was then followed by other research groups.[8−12] In a previous paper,[11] we described the preparation and the photoelectrochemical properties of a series of ruthenium trisbipyridine complexes containing one bipyridine unit substituted by two phosphonic acid groups. The action spectra of some of these dyes demonstrated quite high IPCE values on the metal−ligand charge transfer (MLCT) absorption bands, although the efficiency was limited to wavelengths below 600 nm. In an effort to extend the red photoactivity of this type of dye, we undertook the preparation of a series of complexes responding to the general formula RuL_2X_2, with L = 4,4′-bis(phosphonic acid)-2,2′-bipyridine or 5,5′-bis(phosphonic acid)-2,2′-bipyridine and X = Cl, CN, or SCN. The anchoring group is an important parameter to consider in the design of efficient sensitizers because it may affect both the stability of the linkage and the electronic coupling between the dye and the semiconductor.[13] These factors are expected to have a deep impact on the life span and efficiency of the cell. In addition, the electronic properties of the chromophoric ligands can be modified by the anchoring functionalities and, consequently, those of the corresponding dye sensitizer.[14] We have tried, therefore, to understand on a theoretical basis how the substitution of the carboxylic acid with phosphonic acid functions may affect the spectroscopic properties of the different dyes. Although a number of ruthenium dyes containing chromophoric ligands with phosphonic acid functions have been reported in the literature,[6−12] this is the first study addressing this issue.

We report here a reliable strategy for the preparation of cis ruthenium complexes with coordinated bipyridine bisphosphonate ligands. The complexes have been characterized by UV−vis absorption and emission spectroscopy and electrochemistry, and the photoelectrochemical properties have been studied in sandwich-type TiO_2 photoelectrochemical cells. Their properties have been compared to those of the analogue complexes containing carboxylic acid groups. Molecular orbital (MO) calculations have been performed, and the electronic structures obtained from DFT calculations allow the rationalization of the spectroscopic changes induced by substitution of the carboxylic acids with phosphonic acids functions. The absorption spectra have been analyzed in the framework of the time-dependent density functional theory (TDDFT) formalism.

Experimental Section

General Methods. ^{1}H NMR spectra were recorded on a ASPEC Bruker 200 spectrometer. Chemical shifts are referenced relative to TMSP (trimethylsilylproprionic acid, sodium salt) as an internal standard reference ($\delta = 0$ ppm) for D_2O samples or to the residual protium of the deuterated solvent for methanol ($\delta = 4.5$ ppm). The peak assignments are given as chemical shifts with the number of protons involved and the multiplicity of the signal (s, singlet; d, doublet; t, triplet; m, multiplet) in parentheses.

Thin-layer chromatography (TLC) was carried out on aluminum sheets precoated with Merck 5735 Kiselgel $60F_{254}$. Column chromatography was performed on Merck 5735 Kieselgel 60F (0.040−0.063 mm mesh). Air sensitive reactions were carried out under argon in dry solvents and glassware. Solvents were carefully distilled prior to their uses with standard drying procedures. UV−vis absorption spectra were recorded on UV-2401PC Shimadzu and Perkin-Elmer Lamba 40 spectrophotometers. Fast atom bombardment mass spectroscopy (FAB-MS) analyses were performed in *m*-nitrobenzyl alcohol matrix (MBA) on a ZAB−HF−FAB spectrometer.

Cyclic voltammetric (CV) measurements were performed with a potentiostat-galvanostat MacLab model ML160 controlled by resident software (Echem v1.5.2 for Windows). Solutions for CV measurements in 0.1 N H_2SO_4 were approximately 2 mM before use and were purged with argon in a three-electrode cell. In all the measurements, the working electrode was a carbon paste electrode with a platinum wire as auxiliary electrode. Potentials are compared

(4) (a) Kuciauskas, D.; Freund, M. S.; Gray, H. B.; Winkler, J. R.; Lewis, N. S. *J. Chem. Phys. B* **2001**, *105*, 392−403. (b) Sauve, G.; Cass, M. E.; Doig, S. J.; Lauermann, I.; Pomykal, K.; Lewis, N. S. *J. Chem. Phys. B* **2000**, *104*, 3488−3491. (c) Sauve, G.; Cass, M. E.; Coia, G.; Doig, S. J.; Lauermann, I.; Pomykal, K. E.; Lewis, N. S. *J. Chem. Phys. B* **2000**, *104*, 6821−6836.

(5) (a) Guerrero, G.; Mutin, P. H.; Vioux, A. *Chem. Mater.* **2001**, *13*, 4367−4373. (b) Olivera-Pastor, P.; Maireles-Torres, P.; Rodriguez-Castellon, E.; Jiménez-Lopez, A. *Chem. Mater.* **1996**, *8*, 1758−1769.

(6) Grätzel, M.; Kohle, O.; Nazeeruddin, M. K.; Pechy, P.; Rotzinger, F. P.; Ruile, S.; Zakeeruddin, S. M. In *PCT Int. Appl.*; Ecole Polytechnique Federale de Lausanne, Switz.: WO 95 29, 924, Nov. 1995; 52 pp.

(7) (a) Pechy, P.; Rotzinger, F. P.; Nazeeruddin, M. K.; Kohle, O.; Zakeeruddin, S. M.; Humphry-Baker, R.; Grätzel, M. *Chem. Commun.* **1995**, 65−66. (b) Bonhote, P.; Moser, J. E.; Vlachopoulos, N.; Walder, L.; Zakeeruddin, S. M.; Humphry-Baker, R.; Pechy, P.; Grätzel, M. *Chem. Commun.* **1996**, 1163−1164. (c) Bonhote, P.; Moser, J.-E.; Humphry-Baker, R.; Vlachopoulos, N.; Zakeeruddin, S. M.; Walder, L.; Grätzel, M. *J. Am. Chem. Soc.* **1999**, *121*, 1324−1336. (d) Ruile, S.; Kohle, O.; Pechy, P.; Grätzel, M. *Inorg. Chim. Acta* **1997**, *261*, 129−140. (e) Zakeeruddin, S. M.; Nazeeruddin, M. K.; Pechy, P.; Rotzinger, F. P.; Humphry-Baker, R.; Kalyanasundaram, K.; Grätzel, M.; Shklover, V.; Haibach, T. *Inorg. Chem.* **1997**, *36*, 5937−5946.

(8) (a) Andersson, A.-M.; Isovitsch, R.; Miranda, D.; Wadhwa, S.; Schmehl, R. H. *Chem. Commun.* **2000**, 505−506. (b) Yan, S. G.; Hupp, J. T. *J. Phys. Chem.* **1996**, *100*, 6867−6870. (c) Merrins, A.; Kleverlaan, C.; Will, G.; Rao, S. N.; Scandola, F.; Fitzmaurice, D. *J. Phys. Chem. B* **2001**, *105*, 2998−3004. (d) Zaban, A.; Ferrere, S.; Gregg, B. A. *J. Phys. Chem. B* **1998**, *102*, 452−460. (e) Yan, S. G.; Prieskorn, J. S.; Kim, Y.; Hupp, J. T. *J. Phys Chem. B* **2000**, *104*, 10871−10877.

(9) Montalti, M.; Wadhwa, S.; Kim, W. Y.; Kipp, R. A.; Schmehl, R. H. *Inorg. Chem.* **2000**, *39*, 76−84.

(10) (a) Trammell, S. A.; Moss, J. A.; Yang, J. C.; Nakhle, B. M.; Slate, C. A.; Odobel, F.; Sykora, M.; Erickson, B. W.; Meyer, T. J. *Inorg. Chem.* **1999**, *38*, 3665−3669.

(11) Gillaizeau-Gauthier, I.; Odobel, F.; Alebbi, M.; Argazzi, R.; Costa, E.; Bignozzi, C. A.; Qu, P.; Meyer, G. J. *Inorg. Chem.* **2001**, *40*, 6073−6079.

(12) (a) Trammell, S. A.; Wimbish, J. C.; Odobel, F.; Gallagher, L. A.; Narula, P. M.; Meyer, T. J. *J. Am. Chem. Soc.* **1998**, *120*, 13248−13249. (b) Trammell, S. A.; Yang, J.; Sykora, M.; Fleming, C. N.; Odobel, F.; Meyer, T. J. *J. Chem. Phys. B* **2001**, *105*, 8895−8904.

(13) (a) Asbury, J. B.; Hao, E.; Wang, Y.; Lian, T. *J. Chem. Phys. B* **2000**, *104*, 11957−11964. (b) Sayama, K.; Sugihara, H.; Arakawa, H. *Chem. Mater.* **1998**, *10*, 3825−3832. (c) Schnadt, J.; Bruehwiler, P. A.; Patthey, L.; O'Shea, J. N.; Soedergren, S.; Odelius, M.; Ahuja, R.; Karis, O.; Baessler, M.; Persson, P.; Siegbahn, H.; Lunell, S.; Martensson, N. *Nature* **2002**, *418*, 620−623.

(14) (a) Hou, Y.-J.; Xie, P.-H.; Zhang, B.-W.; Cao, Y.; Xiao, X.-R., Wang, W.-B. *Inorg. Chem.* **1999**, *38*, 6320−6322. (b) Pichot, F.; Beck, J. H.; Elliot, C. M. *J. Chem. Phys. A* **1999**, *103*, 6263−6267. (c) Gholamkhass, B.; Koike, K.; Negishi, N.; Hori, H.; Takeuchi, K. *Inorg. Chem.* **2001**, *40*, 756−765.

to a saturated calomel electrode (SCE). In all the experiments the scan rate was 100 mV/s.

Steady-state luminescence studies were performed using a Yvon Spex Fluoromax 2 spectrofluorimeter equipped with a R3896 Hamamatsu tube. Emission lifetimes were measured with a laser flash photolysis apparatus consisting of a Continuous Surelite II, Q switched (neodymium/yttrium aluminum garnet) laser (half-width 7 ns). Emission was collected at 90° through an Applied Photophysics monochromator equipped with an R 928 Hamamatsu photomultiplier. The signals were acquired on a 600 MHz Le Croy 9360 digital oscilloscope and elaborated by means of Origin 6 software.

Photoanodes Preparation. TiO_2 colloid solutions were prepared by hydrolysis of titanium isopropoxide, $Ti(OCH_2(CH_3)_2)_4$ (Fluka), of which 50 mL were added dropwise, by means of an addition funnel, to 300 mL of deionized water acidified with 2.1 mL of 65% HNO_3 under vigorous stirring. During the hydrolysis a white precipitate formed. The mixture was stirred for 8 h at 80 °C. During this process the mixture was allowed to concentrate to 120 mL, corresponding to a TiO_2 concentration of 170 g/L. A stable colloidal sol resulted from this procedure. The size of the colloidal particles was ca. 8 nm, and X-ray diffraction analysis showed them to consist of anatase. This solution (50 mL) was heated at 220 °C for 12 h in an autoclave. During this process the nanoparticles grew until they were 50−100 nm in size. After the particles cooled at room temperature, 3 g of Carbowax 2000 (Aldrich) was added to the resulting gel and the mixture was stirred at room temperature for 8 h. The conductive glass was covered on two parallel edges with 3M adhesive tape (ca. 20 μm thick) to control the thickness of the TiO_2 film. The colloid was applied to one edge of the conducting glass and distributed with a glass rod sliding over the tape-covered edges. After air-drying, the electrode was heated in an oven at 450 °C for 30 min in the presence of air. The resulting film thickness was of the order of 6−7 μm.

The sensitizers were dissolved in CH_3OH/H_2O (4:1) and were adsorbed by refluxing this solution for 3 h in the presence of the photoanode. In all cases, ca. 5×10^{-3} M solutions of the complex were used.

Photoelectrochemical measurements were performed in a two-electrode sandwich cell arrangement. Typically 10 μL of electrolyte (0.3 M LiI /0.03 M I_2) in acetonitrile was sandwiched between a TiO_2 photoanode and a counter electrode. A Pt-sputtered conductive glass was employed as counter electrode. The cell was illuminated with a 150 W Xe lamp coupled to an Applied Photophysics high-irradiance monochromator. The irradiated area was 0.5 cm^2. Light excitation was through the FTO glass (ca. 10 Ω/square LOEF) substrate of the photoanode. Photocurrents were measured under short-circuit conditions with a Kontron model DMM 4021 digital electrometer, and the cell was illuminated with a 500 W halogen lamp. Incident irradiance was measured with a calibrated silicon photodiode from UDT Technologies.

Chemicals were purchased from Aldrich and used as received. $RuCl_2(DMSO)_4$,[15] 4,4′-bis(ethyl ester phosphonate)-2,2′-bipyridine,[16] and 5,5′-bis(ethyl ester phosphonate)-2,2′-bipyridine[16] were synthesized using literature procedures.

Computational Study. All theoretical calculations were carried out using a Becke's three-parameter hybrid functional[17] with LYP correlation functional[18] (B3LYP), as implemented in the Gaussian98 program.[19] A LanL2DZ effective core potential basis set was employed for all atoms.[20] The theoretical electronic spectra were simulated from the energy of the excited states and transition oscillator strengths calculated by the TDDFT formalism as implemented in the Gaussian98 program.[21] A value equal to 2000 cm^{-1} for the bandwidth at half height has been used in these simulations with Gaussian line shapes because this value often provides us with molar extinction coefficient values of the same order of magnitude as the experimental ones (as it has been checked on several simple complexes).

Preparations. General Procedure for the Complexation of the Ligands 1 and 2. To a solution of bis(ethyl ester phosphonate)-bipyridine **1** or **2** (200 mg, 0.636 mmol) and LiCl (286 mg, 6.8 mmol) in dry DMF (10 mL) in a Schlenk tube was added 205 mg (0.423 mmol) of $Ru(DMSO)_4Cl_2$. The mixture was degassed by pumping and flushing with argon on the vacuum line and then heated at 160−170 °C for 6 h in the dark. After the solution was cooled to room temperature, dichloromethane was added and the precipitate was filtered and washed with dichloromethane. After the compound was dried in a vacuum, the complex was used as such in the next step (average yield 80%).

^{1}H NMR spectrum of the crude complex showed that the original diethyl phosphonate ester groups had been partly hydrolyzed during the course of the reaction because the ethyl ester group's signal integrated for half of the expected value and the peak was shielded (3.8 ppm) compared to the value found in complexes **3** or **4** (4.1 ppm).

General Procedure for Esterification of the Complexes. To a solution of the above complex (203 mg, 0.221 mmol) in oxalyl chloride (2 mL) under argon was carefully added anhydrous DMF (0.3 mL) (during the addition copious gas was evolved). The mixture was then heated at 55−60 °C overnight. The solvents were removed by rotary evaporation, and the crude solid was dried under vacuum. Dry dichloromethane (2 mL) was then added, and the reaction was stirred for 1 h at room temperature. After removal of the solvent by rotary evaporation, freshly distilled EtOH (2 mL) was then added and the mixture was stirred for 3 h at room temperature. After removal of the solvent by rotary evaporation and drying under a vacuum, the crude residue was purified by column chromatography on silica gel and eluted with pure acetone and then with increasing gradients of methanol in acetone (starting from acetone/methanol 2:8 until 3:7).

***cis*-Dichlorobis(4,4′-bis(ethyl ester)phosphonate)-2,2′-bipyridine)ruthenium, 3.** Blue solid, 62% yield. ^{1}H NMR (400 MHz, CD_3OD): δ 10.18 (dd, J = 8.0 Hz and J = 4.0 Hz, 2H, $H_{6'}$), 8.91 (d, J_{H-P} = 16.0 Hz, 2H, $H_{3'}$), 8.74 (d, J_{H-P} = 16.0 Hz, 2H, $\mathbf{H_3}$),

(15) Evans, I. P.; Spencer, A.; Wilkinson, G. *J. Chem. Soc., Dalton Trans.* **1973**, 204−209.
(16) Penicaud, V.; Odobel, F.; Bujoli, B. *Tetrahedron Lett.* **1998**, *39*, 3689−3692.
(17) Becke, A. D. *J. Chem. Phys.* **1993**, *98*, 5648.
(18) Lee, C.; Yang, W.; Parr, R. G. *Phys. Rev. B* **1988**, *37*, 785.
(19) Frisch, M. J.; Trucks, G. W.; Schlegel, H. B.; Scuseria, G. E.; Robb, M. A.; Cheeseman, J. R.; Zakrzewski, V. G.; Montgomery, J. A., Jr.; Stratmann, R. E.; Burant, J. C.; Dapprich, S.; Millam, J. M.; Daniels, A. D.; Kudin, K. N.; Strain, M. C.; Farkas, O.; Tomasi, J.; Barone, V.; Cossi, M.; Cammi, R.; Mennucci, B.; Pomelli, C.; Adamo, C.; Clifford, S.; Ochterski, J.; Petersson, G. A.; Ayala, P. Y.; Cui, Q.; Morokuma, K.; Malick, D. K.; Rabuck, A. D.; Raghavachari, K.; Foresman, J. B.; Cioslowski, J.; Ortiz, J. V.; Stefanov, B. B.; Liu, G.; Liashenko, A.; Piskorz, P.; Komaromi, I.; Gomperts, R.; Martin, R. L.; Fox, D. J.; Keith, T.; Al-Laham, M. A.; Peng, C. Y.; Nanayakkara, A.; Gonzalez, C.; Challacombe, M.; Gill, P. M. W.; Johnson, B. G.; Chen, W.; Wong, M. W.; Andres, J. L.; Head-Gordon, M.; Replogle, E. S.; Pople, J. A. *Gaussian 98*, revision x.x; Gaussian, Inc.: Pittsburgh, PA, 1998.
(20) (a) T. H. Dunning, J.; Hay, P. J. In Plenum Press: 1977; Vol. 2, pp 1−28. (b) Hay, P. J.; Wadt, W. R. *J. Chem. Phys.* **1985**, *82*, 284. (c) Hay, P. J.; Wadt, W. R. *J. Chem. Phys.* **1985**, *82*, 270. (d) Hay, P. J.; Wadt, W. R. *J. Chem. Phys.* **1985**, *82*, 299.
(21) Casida, M. E.; Jamorski, C.; Casida, K. C.; Salahub, D. R. *J. Chem. Phys.* **1998**, *108*, 4439.

8.1 (dd, J_{H-P} = 12.0 Hz and J = 8.0 Hz, 2H, $H_{5'}$), 7.95 (dd, J = 8.0 Hz and J = 4.0 Hz, 2H, H_6), 7.41 (dd, J_{H-P} = 12.0 Hz and J = 8.0 Hz, 2H, H_5), 4.35 (m, 8H, OCH_2CH_3), 4.19 (m, 8H, OCH_2CH_3), 1.47 (t, J = 4.0 Hz, 12H, OCH_2CH_3), 1.33 (t, J = 4.0 Hz, 12H, OCH_2CH_3). ^{13}C NMR (100 MHz D_2O/NaOD): δ 161.8, 159.9, 155.5, 155.3, 137.8 (d, J = 125 Hz), 135.9 (d, J = 125 Hz), 128.8 (d, J = 8 Hz), 128.6 (d, J = 8 Hz), 126.3 (d, J = 8 Hz), 126.1 (d, J = 8 Hz), 65.5 (d, J = 18 Hz), 65.4 (d, J = 18 Hz), 17.0 (d, J = 8 Hz), 16.9 (d, J = 8 Hz). MS-FAB (m/z) calcd for $C_{36}H_{52}Cl_2N_4O_{12}P_4Ru$, 1028.10; found, 1028.1.

***cis*-Dichlorobis(5,5′-bis(ethyl ester)phosphonate)-2,2′-bipyridine)ruthenium, 4.** Dark blue solid, 70% yield. ^{1}H NMR (400 MHz, CD_3OD) δ: 10.42 (dd, J_{H-P} = 16.8 Hz and J = 3.0 Hz, 2H, $H_{6'}$), 8.88 (dd, J_{H-P} = 16.5 Hz and J = 7.0 Hz, 2H, $H_{3'}$), 8.71 (dd, J_{H-P} = 16.5 Hz and J = 7.0 Hz, 2H, H_3), 8.46 (ddd, J_{H-P} = 20.1 Hz, J = 16.5 Hz and J = 3.4 Hz, 2H, $H_{4'}$), 8.07 (ddd, J_{H-P} = 20.1 Hz, J = 16.5 Hz and J = 3.4 Hz, 2H, H_4), 7.91 (dd, J = 16.8 Hz and J = 3.0 Hz, 2H, H_6), 4.32 (m, 8H, OCH_2CH_3), 4.03 (m, 8H, OCH_2CH_3), 1.43 (t, J = 14.0 Hz, 12H, OCH_2CH_3), 1.25 (t, J = 14.0 Hz, 12H, OCH_2CH_3). ^{13}C NMR (100 MHz (D_2O/NaOD): δ 162.7, 160.3, 155.9, 155.6, 138.1, 136.0, 128.6, 126.6, 123.3 (d, J = 19 Hz), 123.1 (d, J = 19 Hz), 63.7 (d, J = 22 Hz), 63.4 (d, J = 22 Hz), 16.2. MS-FAB (m/z) calcd for $C_{36}H_{52}Cl_2N_4O_{12}P_4Ru$, 1028.10; found, 1028.1.

General Procedure for Complete Hydrolysis of the Diethyl Ester Phosphonate. A solution of *cis*-dichloro bis(bis(ethyl ester phosphonate)-2,2′-bipyridine)ruthenium (218 mg, 0.212 mmol) in 10 mL of 6 N HCl was refluxed for 18 h. After this period, the solvent was evaporated on a rotary evaporator. The resulting purple solid was then dissolved in a minimal amount of water and purified by column chromatography using Sephadex LH20 (25 g packed in a column h = 29 cm, d = 20 mm) as stationary phase and water as eluent. The major purple band was collected and corresponds to the desired complex.

***cis*-Dichlorobis(4,4′-bis(phosphonic acid)-2,2′-bipyridine)ruthenium, 5.** Purple solid, 82% yield. ^{1}H NMR (400 MHz D_2O/NaOD): δ 9.25 (d, J = 5.6 Hz, 2H, $H_{6'}$), 8.63 (d, J_{H-P} = 12.0 Hz, 2H, $H_{3'}$), 8.44 (d, J_{H-P} = 12.0 Hz, 2H, H_3), 7.88 (dd, J_{H-P} = 12.0 Hz and J = 5.6 Hz, 2H, $H_{5'}$), 7.62 (d, J = 5.6 Hz, 2H, H_6), 7.09 (dd, J_{H-P} = 12.0 Hz and J = 5.6 Hz, 2H, H_5). Anal. Calcd for $C_{20}H_{20}Cl_2N_4O_{12}P_4Ru\cdot 1H_2O$: C, 29.2; H, 2.7; N, 6.8. Found: C, 29.2; H, 2.8; N, 6.7.

***cis*-Dichlorobis(5,5′-bis(phosphonic acid)-2,2′-bipyridine)ruthenium, 6.** Purple solid, 86% yield. ^{1}H NMR (400 MHz D_2O/NaOD): δ 9.46 (d, J_{H-P} = 7.6 Hz, 2H, $H_{6'}$), 8.40 (d, J = 8.0 Hz, 2H, $H_{3'}$), 8.20 (d, J = 8.0 Hz, 2H, H_3), 8.19 (dd, J_{H-P} = 9.6 Hz and J = 9.6 Hz, 2H, $H_{4'}$), 7.88 (d, J_{H-P} = 7.6 Hz, 2H, H_6), 7.74 (dd, J_{H-P} = 9.6 Hz and J = 9.6 Hz, 2H, H_4). Anal. Calcd for $C_{20}H_{20}Cl_2N_4O_{12}P_4Ru\cdot 6H_2O$: C, 26.3; H, 3.5; N, 6.1. Found: C, 26.4; H, 3.6; N, 5.9.

General Procedure for the Preparation of the Dicyano Complexes. *cis*-Dichlorobis(diphosphonic acid bipyridine)ruthenium (50 mg, 0.058 mmol) and KCN (65 mg, 1.0 mmol) were dissolved in a mixture of water (5 mL) and methanol (5 mL) in a round-bottomed flask, and then the solution was purged with argon. The flask was then covered with aluminum foil and heated at reflux for 12 h in the dark. After the flask cooled to room temperature, acetone was added to the crude reaction mixture and the precipitate was filtered off and washed with acetone. The resulting purple solid was then dissolved in a minimum amount of water and purified by column chromatography using Sephadex LH20 as stationary phase and water as eluent.

***cis*-Dicyanobis(4,4′-bis(phosphonic acid)-2,2′-bipyridine)ruthenium, 7.** Orange solid, 83% yield. ^{1}H NMR (400 MHz D_2O/NaOD): δ 9.39 (dd, J = 6.0 Hz, J = 3.0 Hz, 2H, $H_{6'}$), 8.61 (d, J_{H-P} = 11.0 Hz, 2H, $H_{3'}$), 8.54 (d, J_{H-P} = 11.0 Hz, 2H, H_3), 7.83 (dd, J_{H-P} = 11.0 Hz and J = 5.0 Hz, 2H, $H_{5'}$), 7.62 (dd, J = 5.0 Hz, J = 3.0 Hz, 2H, H_6), 7.41 (dd, J_{H-P} = 10.5 Hz and J = 5.6 Hz, 2H, H_5). ^{13}C NMR (100 MHz D_2O/NaOD): δ 169.10 (CN), 159.05, 158.05, 156.65 (d, J = 10 Hz), 154.40 (d, J = 80 Hz), 152.80 (d, J = 80 Hz), 151.35 (d, J = 10 Hz), 130.35 (d, J = 10 Hz), 129.85 (d, J = 10 Hz), 126.85 (d, J = 10 Hz), 126.25 (d, J = 10 Hz). IR (KBr) ν(CN) at 2068.7 cm^{-1}. Anal. Calcd for $C_{22}H_{20}N_6O_{12}P_4Ru\cdot 2H_2O$: C, 30.1; H, 3.0; N, 10.5. Found: C, 30.0; H, 3.0; N, 10.4.

***cis*-Dicyanobis(5,5′-bis(phosphonic acid)-2,2′-bipyridine)ruthenium: 8.** Orange solid, 80% yield. ^{1}H NMR (400 MHz D_2O/NaOD): δ 9.61 (d, J_{H-P} = 6.8 Hz, 2H, $H_{6'}$), 8.41 (d, J = 8.0 Hz, 2H, $H_{3'}$), 8.32 (d, J = 8.0 Hz, 2H, H_3), 8.28 (dd, J_{H-P} = 9.0 Hz and J = 9.0 Hz, 2H, $H_{4'}$), 8.10 (dd, J_{H-P} = 9.0 Hz and J = 9.0 Hz, 2H, H_4), 7.86 (d, J_{H-P} =10 Hz, J = 6.8 Hz, 2H, H_6). ^{13}C NMR (100 MHz D_2O/NaOD): 169.60 (CN), 159.30, 158.45 (d, J = 10 Hz), 158.00, 153.15 (d, J = 10 Hz), 142.55 (d, J = 70 H), 141.90 (d, J = 10 Hz), 141.20 (d, J = 10 Hz), 140.95 (d, J = 70 Hz,), 125.75 (d, J = 10 Hz), 125.05 (d, J = 10 Hz). IR (KBr) ν(CN) at 2063.6 cm^{-1}. Anal. Calcd for $C_{22}H_{20}N_6O_{12}P_4Ru\cdot 4H_2O$: C, 28.8; H, 3.4; N, 10.1. Found: C, 28.8; H, 3.5; N, 10.2.

General Procedure for the Preparation of the Thiocyanate Complexes. *cis*-Dichlorobis(diphosphonic acid bipyridine)ruthenium (50 mg, 0.086 mmol) and KSCN (85 mg, 0.87 mmol) were dissolved in a mixture of water (5 mL) and ethanol (5 mL) in a flask, and the mixture was purged with argon. The flask was then covered with aluminum foil and heated at reflux for 12 h in the dark. After the flask cooled to room temperature, acetone was added to the crude reaction mixture and the precipitate was filtered off and washed with acetone. The resulting purple solid was then dissolved in a minimum amount of water and purified by column chromatography using Sephadex LH20 as stationary phase and water as eluent.

***cis*-Dithiocyanatobis(4,4′-bis(phosphonic acid)-2,2′-bipyridine)-ruthenium, 9.** Dark blue solid, 91% yield. ^{1}H NMR (400 MHz D_2O/NaOD) δ: 9.44 (dd, J = 11.0 Hz, J = 6.0 Hz, 2H, $H_{6'}$); 8.74 (d, J_{H-P} = 12.0 Hz, 2H, $H_{3'}$), 8.58 (d, J_{H-P} = 12.0 Hz, 2H, H_3), 8.01 (dd, J_{H-P} = 20.1 Hz and J = 12.0 Hz, 2H, $H_{5'}$), 7.73 (dd, J = 11.0 Hz, J = 6.0 Hz, 2H, H_6), 7.34 (dd, J_{H-P} = 20.1 Hz and J = 12.0 Hz, 2H, H_5). ^{13}C NMR (100 MHz D_2O/NaOD): δ 161.15, 161.10, 155.65 (d, J = 10 Hz), 154.85 (d, J = 10 Hz), 148.75 (d, J = 70 Hz), 147.05 (d, J = 70 Hz), 134.90 (SCN), 130.30 (d, J = 10 Hz), 129.30 (d, J = 10 Hz), 126.70 (d, J = 10 Hz), 125.65 (d, J = 10 Hz). IR (KBr) ν(CN) at 2114.4 cm^{-1}. Anal. Calcd for $C_{22}H_{20}N_6O_{12}P_4S_2Ru\cdot 3H_2O$: C, 27.3; H, 3.0; N, 9.6. Found: C, 27.1; H, 3.2; N, 9.5.

***cis*-Dithiocyanatobis(5,5′-bis(phosphonic acid)-2,2′-bipyridine)-ruthenium, 10.** Purple solid, 88% yield. ^{1}H NMR (400 MHz D_2O/NaOD): δ 9.64 (d, J_{H-P} = 7.6 Hz, 2H, $\mathbf{H_{6'}}$), 8.54 (d, J = 8.0 Hz, 2H, $H_{3'}$), 8.38 (dd, J_{H-P} = 9.6 Hz and J = 9.6 Hz, 2H, $H_{4'}$), 8.36 (d, J = 8.0 Hz, 2H, H_3), 8.01 (dd, J_{H-P} = 9.6 Hz and J = 9.6 Hz, 2H, H_4), 7.86 (d, J_{H-P} = 7.6 Hz, 2H, H_6). ^{13}C NMR (100 MHz D_2O/NaOD): δ 162.10, 161.10, 156.75 (d, J = 10 Hz), 155.85 (d, J = 10 Hz), 141.40 (d, J = 10 Hz), 140.50 (d, J = 10 Hz), 139.10 (d, J = 110 Hz), 137.35 (d, J = 110 Hz), 134.50 (SCN), 126.15 (d, J = 10 Hz), 125.85 (d, J = 10 Hz). IR (KBr) ν(CN) at 2117.5 cm^{-1}. Anal. Calcd for $C_{22}H_{20}N_6O_{12}P_4S_2Ru\cdot 5H_2O$: C, 26.2; H, 3.3; N, 9.2. Found: C, 26.1; H, 3.0; N, 9.1.

Scheme 1. Synthetic Route for the Preparation of the Ruthenium Sensitizers Described in This Study

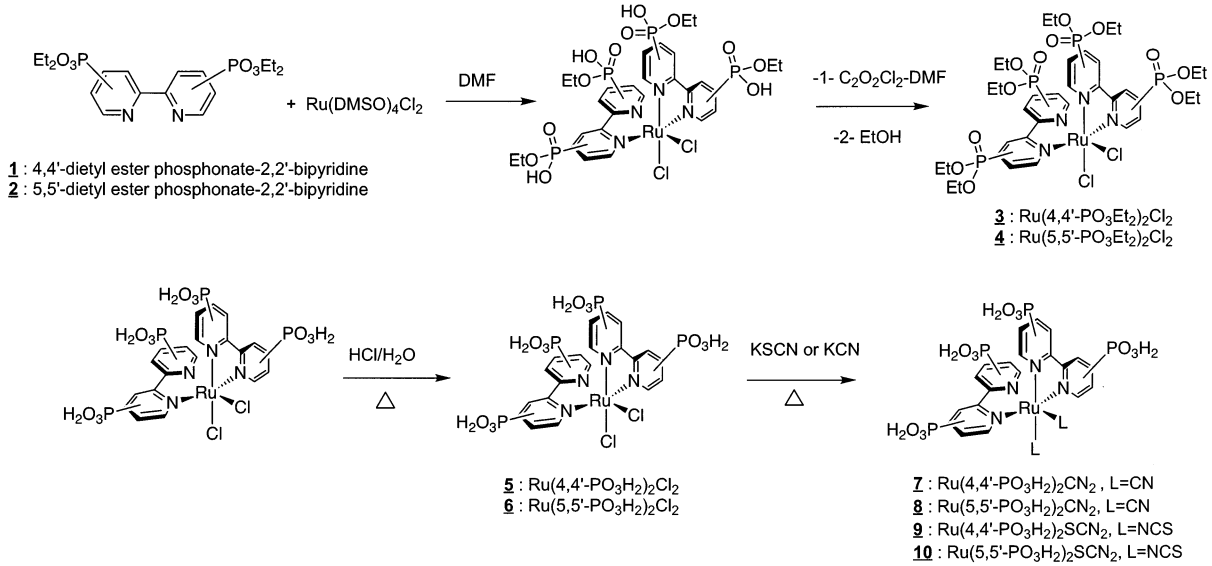

Results and Discussion

Preparations. The investigated complexes are of the general formula *cis*-RuL_2X_2 with L = 2,2′-bipyridine-4,4′-bisphosphonic acid (ligand **1**) or with L′ = 2,2′-bipyridine-5,5′-bisphosphonic (ligand **2**). The preparation of this type of complex usually relies on two steps.[22,23] The first consists of refluxing in DMF 2 equiv of the bidentate ligand L with 1 equiv of ruthenium trichloride to yield a *cis*-ruthenium bischlorobisbipyridine complex (*cis*-RuL_2Cl_2). In the second step, the chloride ligands are substituted by the thiocyanate or cyano ligands. This is achieved by heating in DMF the ruthenium bis-chloro complex with NaSCN or KCN. The preparations of complexes **5** and **9** have been reported by Grätzel et al. in a patent;[6] however, no characterization of these molecules was given and the reported procedure did not permit us to obtain highly pure samples of these species. We have therefore developed a new procedure for the preparation of ruthenium complexes with the phosphonated bipyridine **1** and **2**, which is shown in Scheme 1.

Starting from the phosphonated bipyridine ligands **1** and **2**, the first step was dramatically improved by using the complex $Ru(DMSO)_4Cl_2$ instead of $RuCl_3$ in water. This could be clearly seen from the ^1H NMR spectrum of the crude reaction mixture that indicated a lower amount of impurities when $Ru(DMSO)_4Cl_2$ was used. This can be ascribed to fewer byproduct formations, probably due to the utilization of a ruthenium(II) precursor with weakly binding ligands (DMSO). During the first coordination step, whether the source of ruthenium used was $Ru(DMSO)_4Cl_2$ or $RuCl_3$, nH_2O, the diethyl ester phosphonate groups of complex **3** or **4** were partially hydrolyzed. A purification step was necessary here to remove the tris-bipyridine ruthenium complex formed during the reaction; however, all our attempts of purification, through recrystallization or by column chromatography, failed. In fact the highly polar groups (PO(OH)(OEt)) cause an almost irreversible adsorption on silica or alumina gels even if elution is performed with highly polar mixtures of solvents. The monohydrolyzed phosphonate groups of the complexes **3** or **4** were therefore esterified by a standard procedure using activation of the phosphonate by oxalyl chloride followed by addition of dry ethanol.[24] The resulting compounds could be easily purified by column chromatography. The cis geometry of complexes **3** and **4** was confirmed by NMR spectroscopy (see below). The diethyl ester phosphonate groups were fully hydrolyzed by heating the complexes in hydrochloric acid solution. Chloride ligand exchange with thiocyanato or cyano anions was subsequently performed in water with an excess of the monodentate ligands. Column chromatography on dextran-based Sephadex LH-20 afforded the pure complexes **7**−**10** with good yields. The above complexes were found to be soluble in methanol and water with a larger solubility at basic pH.

NMR and IR Spectroscopic Studies. The NMR spectra of the complexes were measured in D_2O/NaOD solutions to achieve sufficiently large concentrations, compatible with fast spectrum recording and high signal-to-noise ratio. The ^1H NMR spectra of all the complexes show six sharp and well-resolved signals in the aromatic region, corresponding to the six magnetically inequivalent protons of the bipyridine (cf. Figure 1).

The downfield-shifted proton resonance peaks can be assigned to the protons that are close to the second pyridine units, whereas the high-field proton resonances are assigned to the protons that are in the vicinity of the non-bipyridinic ligands. This assignment is based on the assumption that deshielding of the protons can be due to an induced magnetic field created by the ring current circulation on pyridine

(22) Nazeeruddin, M. K.; Liska, P.; Vlachopoulos, N.; Grätzel, M. *J. Am. Chem. Soc.* **1993**, *115*, 6382−6390.
(23) Argazzi, R.; Bignozzi, C. A.; Heimer, T. A.; Castellano, F. N.; Meyer, G. J. *Inorg. Chem.* **1994**, *33*, 5741−5749.
(24) (a) Biller, S. A.; Forster, C.; Gordon, E. M.; Harrity, T.; Scott, W. A.; Ciosek, C. P., Jr. *J. Med. Chem.* **1988**, *31*, 1869−1871. (b) Lorga, B.; Carmichae, D.; Savignac, P. *C. R. Acad. Sci. Ser. IIc: Chim.* **2000**, *3*, 821−829. (c) Rogers, R. S. *Tetrahedron Lett.* **1992**, *33*, 7473−7474.

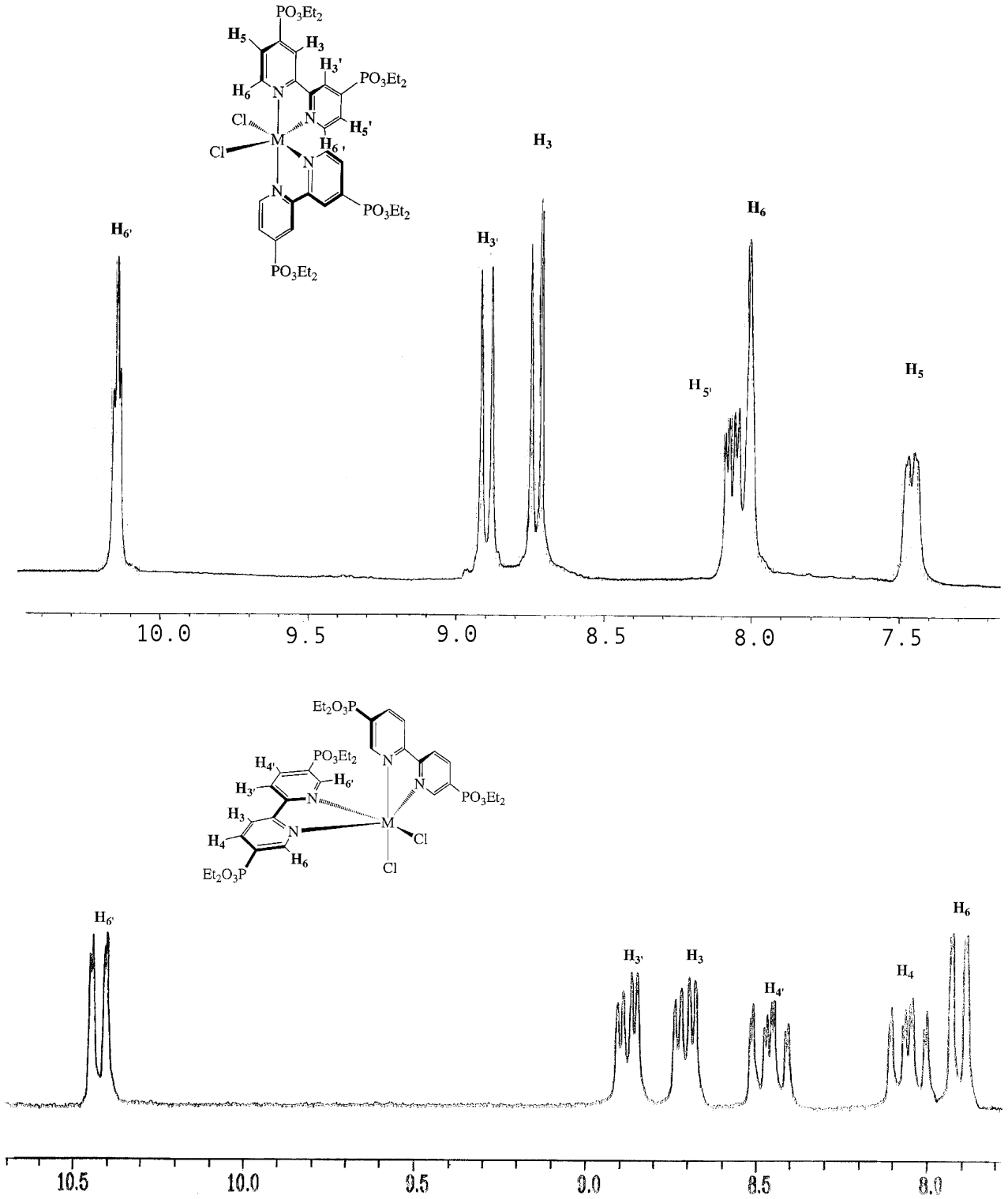

Figure 1. Aromatic region of the ^{1}H NMR spectra of complexes **3** and **4** recorded in CD_3OD.

aromatic moieties. This deshielding is only significant at short distances and therefore affects only protons that are close to the bipyridine. In these cis octahedral complexes, the two bipyridine ligands are equivalent, but the protons of one bipyridine are all inequivalent. In the aliphatic region of the esterified form of the dichloro complexes **3** and **4**, the two phosphonate ethyl ester groups (CH_3 and CH_2 of PO_3Et_2) are also inequivalent and they give rise to four multiplets. Therefore, the observed patterns are in agreement with the cis geometry of the complexes. The trans geometry would have resulted in a simpler NMR spectrum due to the higher symmetry and would have yielded only three peaks in the aromatic region due to the four magnetically equivalent pyridine units.

^{13}C NMR spectra were also recorded because the chemical shift of the thiocyanato ligand is informative of its linkage

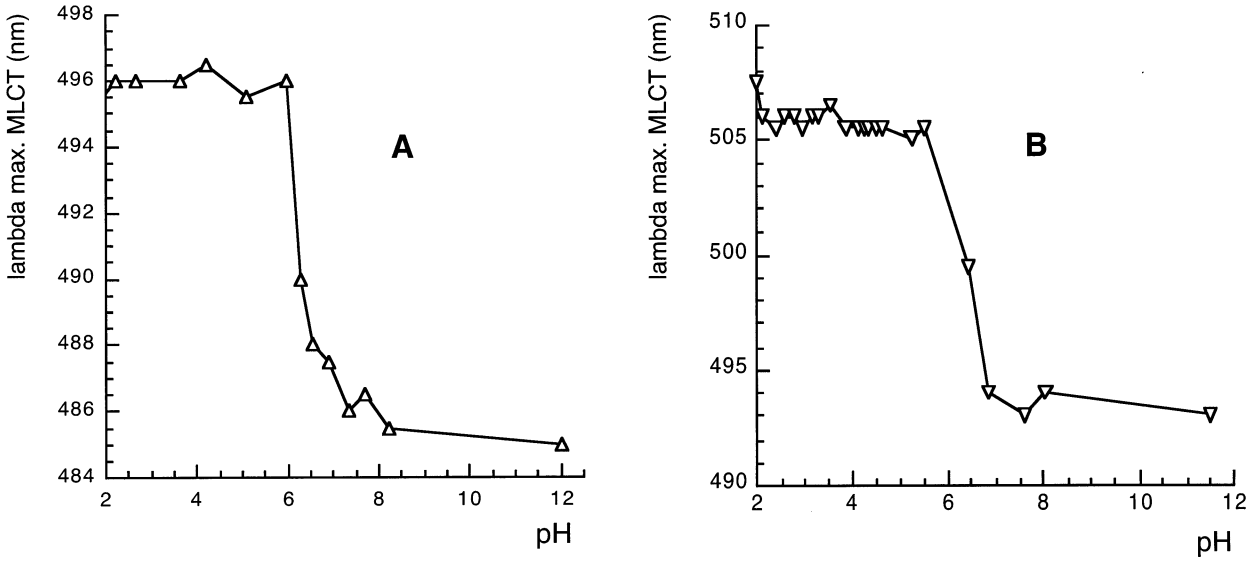

Figure 2. Maximum absorbance of the MLCT transition as a function of the pH. (A) Ru(4,4′-PO_3H_2)$_2$$NCS_2$ (**9**). (B) Ru(5,5′-PO_3H_2)$_2$$NCS_2$ (**10**).

isomerism (N- or S- bound to ruthenium). The ruthenium dichloro complexes **5** and **6** were not sufficiently soluble in basic solution to allow the registration of ^{13}C NMR spectra. The ^{13}C of the S-bound complex displays an upfield-shifted signal in the range of 112−128 ppm, whereas the N-bound is generally downfield-shifted around 130−140 ppm.[25] The ^{13}C chemical shifts of the complexes **9** and **10** are 134.9 and 134.5 ppm, respectively, indicating that the SCN ligand is N-bound in both cases.[25] This is in agreement with the results of Grätzel et al. for related ruthenium complexes.[25,7d] These conclusions are also well supported by IR spectroscopy. IR spectra were recorded in KBr pellets, and the ν_{CN} bands of complexes **9** and **10** were located respectively at at 2114 and 2118 cm^{-1}. From earlier literature results[26] it was demonstrated that this band appears around 2110 cm^{-1} for N-bound thiocyanate, whereas it was shifted to lower energy for the S-bound complexes (ca. 2056 cm^{-1}).

Determination of the pK_a Values of the Phosphonic Acid Group by UV−vis Titration. The MLCT absorption bands of the investigated complexes are very sensitive to pH variations due to the dissociation of the phosphonic acid groups. Deprotonation of the phosphonic acid groups causes an eye-discernible color change of the solution, which is characterized by a blue shift of the MLCT absorption band. The pK_a values were determined by plotting the maximum absorbance wavelength corresponding to the lowest energy MLCT band as a function of the pH of the solution. Representative titration curves are shown in Figure 2. The first dissociation constant pK_{a1} (below pH 2) could not be resolved because of the limit of detection of the pH meter at low pH values. However, for complexes **9** and **10**, pK_{a2} values of 6.0 and 6.1 could be unambiguously determined by this method. The titration curves show a single pK_a titration point, indicating that the four phosphonic acid groups dissociate simultaneously at the same or at very close pH values. The pK_a values obtained in this work are in agreement with those reported by the groups of Grätzel[27] and Schmehl.[9]

Electronic Absorption Spectra. For the purpose of having only one species in solution (one protonation state of the phosphonic acid groups), the electronic absorption spectra of the complexes were recorded in 0.1 N sulfuric acid solutions in water. In such conditions, the dissociation of the phosphonic acid groups is expected to be negligible. Protonation of the cyanide ligands is also expected to be negligible in aqueous solution at pH 1.[28] The UV−vis absorption data are summarized in Table 1, and representative absorption spectra are shown in Figures 3 and 4.

The electronic spectra display intense absorption bands ($\epsilon \approx 5 \times 10^4$ M^{-1} cm^{-1}) in the UV region that are attributed to $\pi-\pi^*$ transitions localized on bipyridine ligands. The lower energy band, between 400 and 600 nm, is assigned to dπ(Ru)$-\pi^*$(bpy) ^{1}MLCT transitions. The wavelength of the maximum absorption of this band depends on the ancillary ligand X and on the position of the phosphonic acid groups on the bipyridine ligand (4,4′ or 5,5′). Consistent with previous observations on related ruthenium dyes containing bpy(COOH)$_2$ ligands,[23] the energy of the MLCT bands increases by ca. 90 cm^{-1} following deprotonation of the phosphonic acid functions and decreases by decreasing the π-accepting ability of the ancillary ligand X (CN > NCS > Cl) (cf. Figure 3). The spectra of the complexes containing the 5,5′-diphosphonic acid-2,2′-bipyridine (**4**, **6**, **8**, and **10**) are red shifted with respect to those deriving from the 4,4′-diphosphonic acid-2,2′-bipyridine (**3**, **5**, **7**, and **9**); a further red shift of 70 cm^{-1} (19 nm) and of 120 cm^{-1} (37 nm) is observed following esterification of complexes **5** and **6**, respectively (Table 1). Finally, it is interesting to compare the absorption spectrum of one the most studied and efficient sensitizers, *cis*-Ru(4,4′-COOH)$_2$$NCS_2$ (N3), with its phosphonated analogue, Ru(4,4′-PO_3H_2)$_2$$NCS_2$ (**9**). It can be

(25) Hermann, R.; Grätzel, M.; Nissen, H. U.; Shklover, V.; Nazeeruddin, M. K.; Zakeeruddin, S. M.; Barbe, C.; Kay, A.; Haibach, T.; Steurer, W. *Chem. Mater.* **1997**, *9*, 430−439.
(26) Kohle, O.; Ruile, S.; Grätzel, M. *Inorg. Chem.* **1996**, *35*, 4779−4787.
(27) Nazeeruddin, M. K.; Zakeeruddin, S. M.; Humphry-Baker, R.; Kaden, T. A.; Grätzel, M. *Inorg. Chem.* **2000**, *39*, 4542−4547.
(28) Peterson, S. H.; Demas, J. N. *J. Am. Chem. Soc.* **1979**, *101*, 6571−6576.

Table 1. Spectroscopic and Electrochemical Data of the Complexes

complexes	absorption maxima,[a] nm (ϵ, M^{-1} cm^{-1})	$E_{1/2}(Ru^{III/II})$, V[b]	emission maxima,[d] nm (E_{00}, eV)	emission maxima,[e] nm (E_{00}, eV)	τ [f], ns	$E_{1/2}$* ($Ru^{III/II}$),[g] V
Ru(4,4′-PO_3Et_2)$_2Cl_2$ (**3**)	528 (4400), 379 (4100), 308 (19900)					
Ru(5,5′-PO_3Et_2)$_2Cl_2$ (**4**)	572 (2060), 366 (2600), 302 (26300)					
Ru(4,4′-PO_3H_2)$_2Cl_2$ (**5**)	509 (6120), 364 (6900), 303 (37600)	0.51	Ne[c]	Ne[c]		
Ru(5,5′-PO_3H_2)$_2Cl_2$ (**6**)	535 (2800), 364 (4000), 321 (14900), 302 (34300), 255 (15700)	0.49	Ne[c]	Ne[c]		
Ru(4,4′-PO_3H_2)$_2CN_2$ (**7**)	453 (5600), 297 (31160), 245 (12000)	1.03	635 (2.24)	658 (2.18)	566	−1.15
Ru(5,5′-PO_3H_2)$_2CN_2$ (**8**)	461 (4540), 293 (55300), 250 (19700)	1.02	668 (2.14)	666 (2.14)	103	−1.12
Ru(4,4′PO_3H_2)$_2NCS_2$ (**9**)	494 (7000), 360 (7860), 303 (33960)	0.68[c]	700 (2.12)	743 (2.0)	56	−1.32
Ru(5,5′PO_3H_2)$_2NCS_2$ (**10**)	515 (4730), 351 (5900), 299 (55230), 250 (24460)	0.64[c]	740 (1.99)	763 (1.98)	9.8	−1.34
Ru(4,4′-CO_2H)$_2NCS_2$ (N**3**)	516 (10840), 390 (11500), 315 (42000)	0.70[c]	740 (2)	803 (1.84)	28	−1.14

[a] Recorded in 0.1 N sulfuric acid. [b] Half-wave potentials vs SCE recorded in 0.1 N sulfuric acid. [c] Anodic peak potentials of irreversible process. Ne = no emission. [d] Emission maximum measured for the anionic forms of the complexes at room temperature in deaerated methanol. [e] Emission maximum measured for the protonated forms of the complexes at room temperature in deaerated methanol, excitation was made on the maximum absorption of the MLCT band. [f] Emission lifetimes of the anionic forms of the complexes. [g] Excited-state redox potentials ($E^*(Ru^{III/II})$) calculated according to the equation $E(Ru^{III/II}) = E_{1/2}(Ru^{III/II}) - E_{00}$(MLCT), where E_{00}(MLCT) represents the zero−zero spectroscopic energy, taken at 5% intensity maximum.

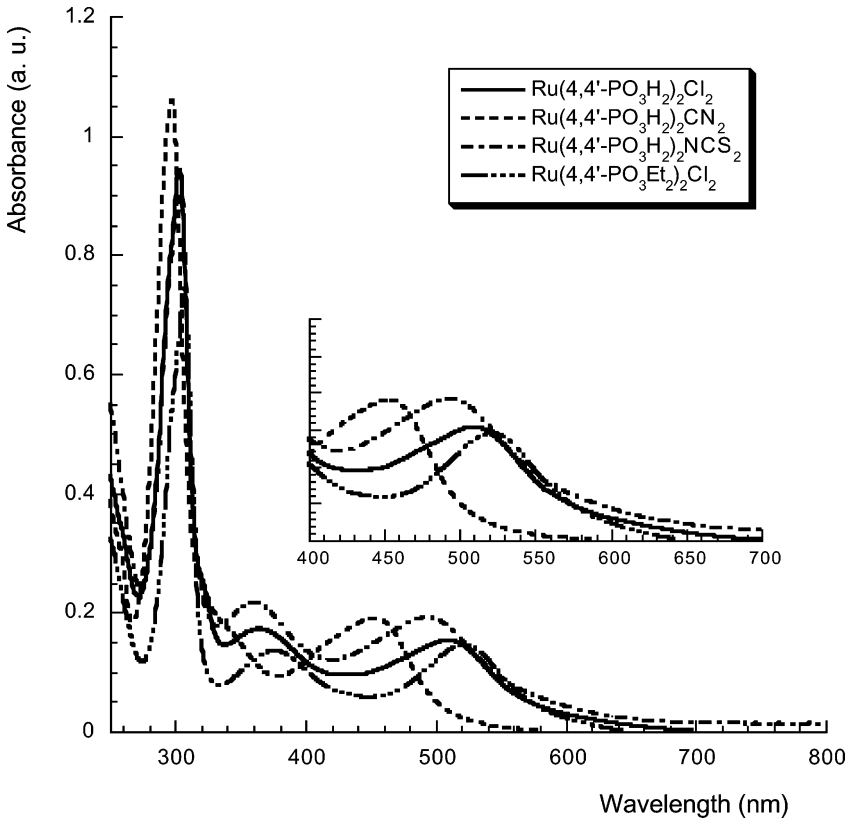

Figure 3. Electronic absorption spectra of some ruthenium complexes recorded in sulfuric acid solution (0.1 N). Ru(4,4′-PO_3H_2)$_2X_2$ where X = Cl (**5**), X = CN (**7**), and X = NCS (**9**) and Ru(4,4′-PO_3Et_2)$_2Cl_2$ (**3**).

observed in Figure 4 that the spectrum of the carboxylated bipyridine complex is slightly red shifted with respect to the phosphonated complex. The changes of the absorption spectral features can be rationalized in terms of MO theory considering the energy of the LUMO and HOMO orbitals of the complexes.

Electrochemical Characterization. The electrochemical properties of the complexes were studied by cyclic voltammetry in 0.1 N H_2SO_4 on carbon paste electrodes. The half-wave potentials ($E_{1/2}$) of the $Ru^{III/II}$ redox couple are reported in Table 1. Half-wave potentials ($E_{1/2}$) were confirmed by square-wave voltammetry (frequency = 15 Hz), and they are in excellent agreement with the values found by cyclic voltammetry for the reversible processes.

Due to the occurrence of the water reduction reaction, the electrochemical study was limited to anodic potentials. The first electrochemical process is a metal-centered oxidation Ru^{III}/Ru^{II} as generally observed for other ruthenium(II) polypyridine complexes.[29] All the dichloro and dicyano complexes display a reversible oxidation process, while electrochemical irreversibility was observed for the NCS-containing species (Figure 5).

(29) Eskelinen, E.; Luukkanen, S.; Haukka, M.; Ahlgren, M.; Pakkanen, T. A. *J. Chem. Soc., Dalton Trans.* **2000**, 2745−2752.

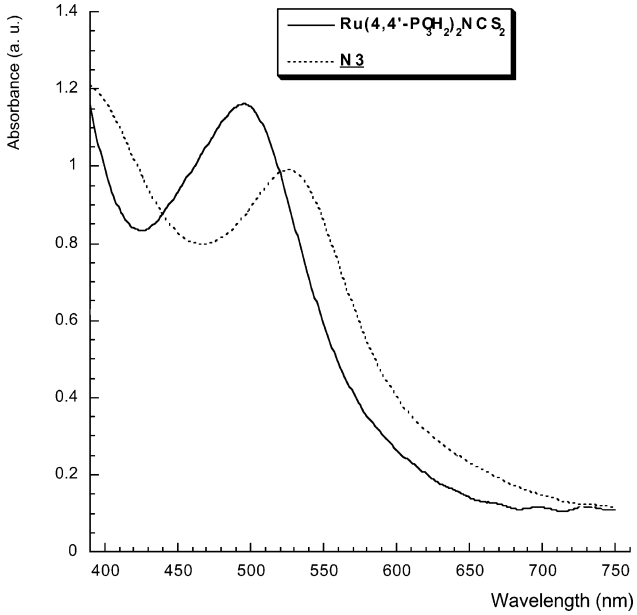

Figure 4. Overlay of the electronic absorption spectra of TiO_2 photoanode stained with $Ru(4,4'\text{-}PO_3H_2)_2NCS_2$ (**9**) and N3.

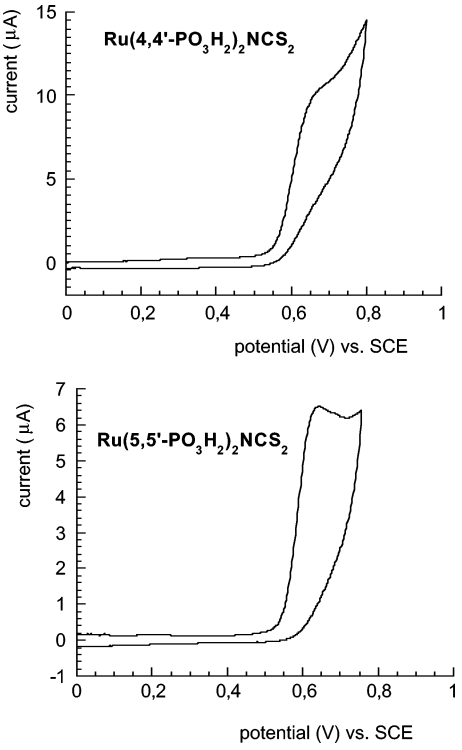

Figure 5. Cyclic voltammograms of complexes $Ru(4,4'\text{-}PO_3H_2)_2NCS_2$ (**9**) and $Ru(5,5'\text{-}PO_3H_2)_2NCS_2$ (**10**) recorded in 0.1 N sulfuric acid at scan rate 100 mV/s.

An analogous behavior was observed for the $Ru(H_2dcb)(NCS)_2$ complex and attributed to charge delocalization between dπ and π NCS orbitals, leading to oxidation of the NCS ligand.[30] Substitution of chloride with cyanide results in a steady increase of $E_{1/2}$ ($Ru^{III/II}$) from 0.6 to 1 V, consistent with well-known differences of the σ-electron-donating/π-accepting properties of these ligands.

Photoelectrochemical Study. The complexes were tested as sensitizers for nanocrystalline TiO_2 solar cells. The incident monochromatic photon to current conversion efficiency (IPCE) collected under short-circuit conditions is shown in Figure 6.

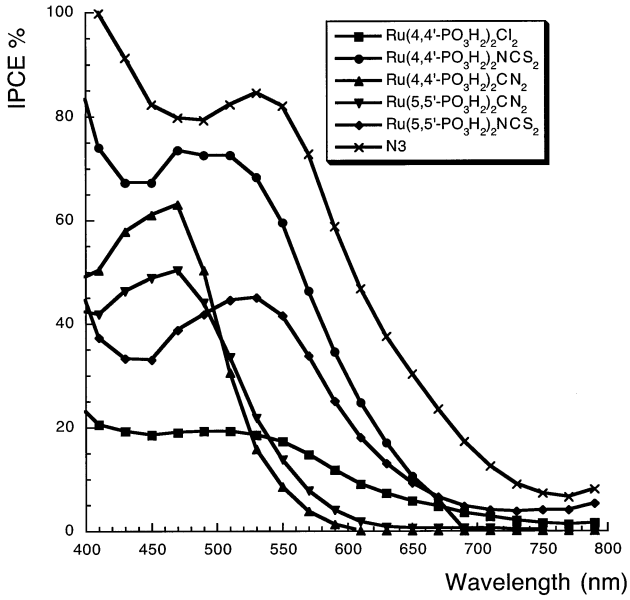

Figure 6. Photoaction spectra (IPCE) of the phosphonated ruthenium complexes **5** (1.7), **7** (0.8), **8** (0,65), **9** (1.2), and **10** (0.7) along with that of N3 (1). The values in parentheses are the optical densities in the MLCT maximum of the investigated photoanodes.

The efficiencies of the sensitizers differ significantly from one another. Optical densities of the photoanodes were in fact in the range 0.65−1.7 (see caption of Figure 6). The highest yields are clearly obtained with the bipyridine ligands bearing the phosphonic acid groups on 4,4′ positions. This has been previously observed by Ferrere[31] and by our groups[11] for other dyes, and it can be most probably rationalized by a difference in the magnitude of the electronic coupling between the sensitizer and the TiO_2 conduction band. Corrections for the optical density of the different electrodes lead to the conclusion that both CN and NCS complexes based on the 4,4′ substituted bipyridine ligand convert almost quantitatively photons into electrons in the visible region (ca. 90−95%), as does the $Ru(H_2dcb)(NCS)_2$ sensitizer. A corrected efficiency of ca. 65% was instead obtained for the corresponding 5,5′-substituted species. The lowest efficiency was exhibited by the 4,4′-substituted dichloro complex with no appreciable photocurent detected from photoanodes loaded with the 5,5′ analogue. This fact can be attributed to the low $E_{1/2}$ $Ru^{III/II}$ values, limiting the driving force for iodide oxidation, as well as to a low charge injection efficiency. The dicyano complexes **7** and **8** yield relatively high IPCE values on the top of the MLCT transition, but IPCE quickly falls to zero at wavelengths above 600 nm due to the weak absorbance above 600 nm.

The photocurrent−voltage curves of the photoelectrochemical cell sensitized with complex **9** and with the N3 sensitizer were recorded in the same experimental conditions.

(30) (a) Cecchet, F.; Gioacchini, A. M.; Marcaccio, M.; Paolucci, F.; Roffia, S.; Alebbi, M.; Bignozzi, C. A. *J. Chem. Phys. B* **2002**, *106*, 3926−3932. (b) Wolfbauer, G.; Bond, A. M.; MacFarlane, D. R. *Inorg. Chem.* **1999**, *38*, 3836−3846.

(31) Ferrere, S. *Chem. Mater.* **2000**, *12*, 1083−1089.

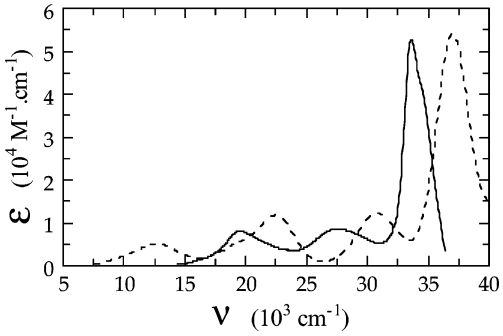

Figure 7. Experimental (solid line) and theoretical (dashed line) spectra for the $Ru(bpy)_2(NCS)_2$ complex. The simulated spectrum corresponds to the optimized geometry and a bandwidth at half-height of 3000 cm^{-1} for the Gaussian line shapes.

The cell sensitized with complex **9** displayed an open-circuit photopotential (V_{OC}) of 490 mV, a short-circuit photocurrent (I_{SC}) of 5 mA/cm^2, and a fill factor (ff) of 0.67, while with the N3 sensitizer the following parameters were obtained: $V_{OC} = 450$ mV, $I_{SC} = 9$ mA/cm^2, and ff = 0.46. The open-circuit photovoltage and the short-circuit photocurrent are lower than those recorded by Grätzel et al.,[3a] because the power of the light source is lower here and the TiO_2 photoanode was not treated with $TiCl_4$. The later treatment decreases the recombination current arising from the reaction of conduction band electrons with triiodite, which is known to decrease both V_{OC} and I_{SC}.[2b] In conclusion, these results indicate that the overall efficiency of the cell sensitized with complex **9** is about 30% lower than that sensitized with the N3, a feature which can be attributed to a lower absorptivity in the red part of the absorption spectrum of the phosphonated dye **9** (cf. Figure 4).

Computational Study. MO calculations were undertaken to rationalize the properties of the new series of complexes and to gain insights on how the anchoring groups modulate their electronic properties. Since bisthiocyanato complexes were found to be the most efficient sensitizers, the calculations were focused on these species. We have first analyzed the influence of the anchoring group on the electronic spectra of $Ru(L)_2(NCS)_2$ complexes. Toward this goal, we have built models of these complexes, taking as a reference the experimental crystal structure of $Ru(bpy)_2(NCS)_2$. The electronic structure of each model has been studied using DFT methods, and the electronic spectra have been simulated from TDDFT calculations.

TDDFT calculations on the model and on the optimized structure of the $Ru(bpy)_2(NCS)_2$ complex lead to similar results. Only slight shifts of the bands in the electronic absorption spectra were found, but the nature of the electronic transitions was not changed. Therefore, we can consider that a less expensive study on models can provide us with qualitatively correct results, even though optimized structures lead to a better agreement with experimental data (cf. Figure 7) Differences with the experimental spectra are probably due to the fact that theoretical calculations are made for isolated molecules and any interaction with the solvent is disregarded. Furthermore, it is noteworthy that in our calculations we have used a pseudopotential basis. The calculated values obtained are without any doubt less accurate than if a more sophisticated basis set was employed.

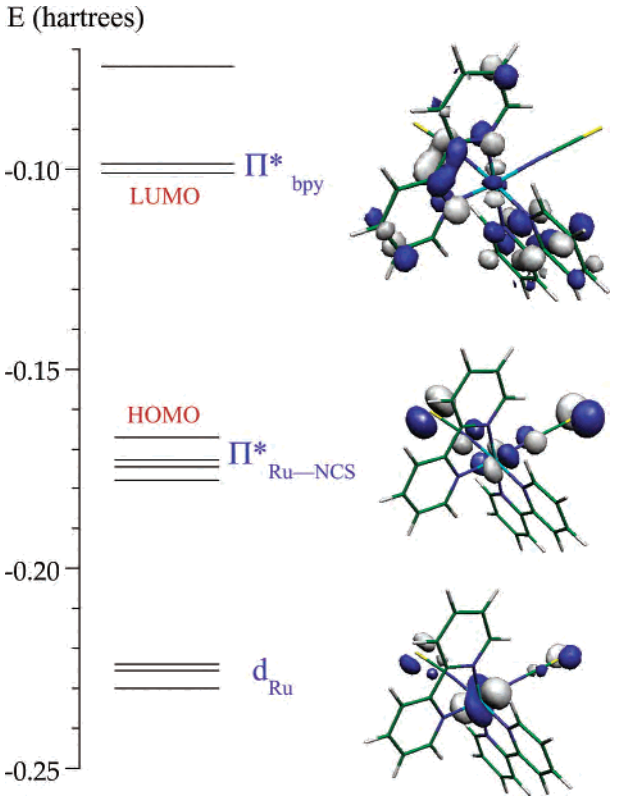

Figure 8. Frontier MOs as obtained in this work for the $Ru(bpy)_2(NCS)_2$ complex. A detailed explanation of the MO nature is developed in the text.

The results of a detailed study of the electronic structure and of the absorption spectrum of the $Ru(bpy)_2(NCS)_2$ complex show that two different groups of higher occupied molecular orbitals (HOMOs) can be considered (cf. Figure 8).

The group located at a higher energy can be described as nonbonding π orbitals mainly centered on the thiocyanate ligands with a very small antibonding contribution from ruthenium metal (Π^*_{Ru-NCS}). The other group of HOMOs, more stable, can be described as t_{2g} Ru orbitals with small contributions from the ligands (d_{Ru}). On the other hand, the closest group of lower unoccupied molecular orbitals (LUMOs) consists mostly of a series of antibonding π orbitals from the bpy ligand (Π^*_{bpy}). It can be expected that these three groups of orbitals will be involved in less energetic electronic transitions. Similar conclusions from the analysis of the electronic transitions have also been found by Siegbahn on the basis of intermediate neglect of differential overlap calculations.[13] Thus, in the calculated spectra three different groups of transitions are observed:

(a) In the low-energy region of spectra ($\lambda > 500$ nm or $\nu < 20\,000$ cm^{-1}, cf. Figures 7 and 8), transitions from Π^*_{Ru-NCS} to Π^*_{bpy} orbitals are found. These transitions can be mostly considered as charge transfers from the thiocyanate group to the L ligand, even though they also show a slight MLCT character. Often, they are neglected in the electronic absorption processes as their intensities are weak, although in some systems they can play an important role. Indeed,

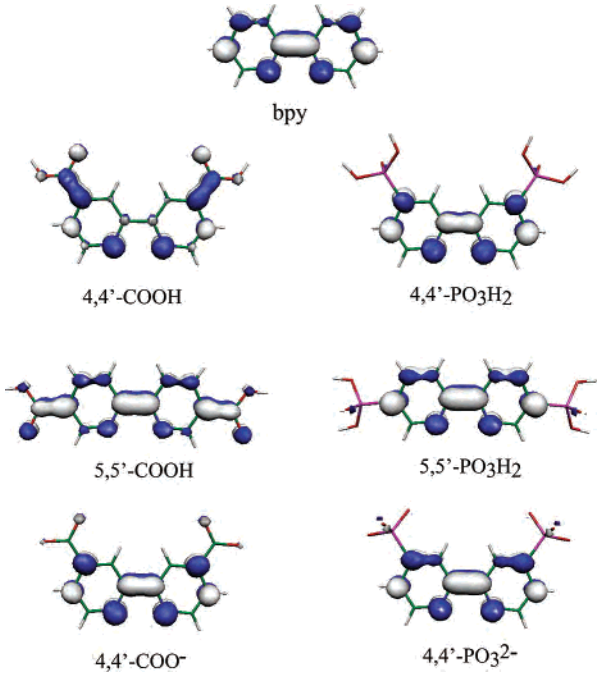

Figure 9. LUMO of the ligands bpy and 4,4′-COOH, 4,4′-PO_3H_2, 5,5′-COOH, 5,5′-PO_3H_2, deprotonated 4,4′-COO^-, and 4,4′-PO_3^{2-} substituted bpy.

one can consider that the proper choice of auxiliary ligands with appropriate orbitals (in terms of energy and symmetry) allows the extension of the absorption spectrum of the complex toward long wavelengths due to this interligand transition.

(b) In the high-energy region (λ < 300 nm or ν > 33 000 cm^{-1}, cf. Figure 7), $\pi-\pi^*$ intraligand transitions are observed, which involve bipyridine-centered orbitals.

(c) In the intermediate-energy region (350−500 nm or 33 000−20 000 cm^{-1}, cf. Figures 7 and 8), more intense MLCT transitions are displayed, where the electron is transferred from the t_{2g} metal orbitals (d_{Ru}) to a π^* orbital mainly localized in the bipyridine ligand (Π^*_{bpy}). In general, these transitions are involved in the energy conversion process of dye sensitizers based on ruthenium complexes.

To understand the energy shift of the MLCT transitions when the bipyridine ligand is functionalized by the carboxylic and phosphonic acid groups, it is crucial to examine how the low-lying unoccupied bpy orbitals are affected by these anchoring groups. The analysis of the ruthenium HOMOs (d_{Ru}) is not so relevant, as they are not so much affected by changes in the bipyridine ligand.

In the carboxylic-substituted bipyridine ligand, the inductive effect of the anchoring group leads to a strong electron density delocalization in the π^* LUMO and consequently to a more stable balance between the bonding and antibonding contributions. As a result, the energy of this orbital decreases and the MLCT transition is observed at lower energy (cf. Figure 9 and Table 2). This effect is reduced when there is a loss of coplanarity between the bpy and the carboxylic groups. On the other hand, the LUMO of bpy presents a greater electron density in 5 and 5′ than in 4 and 4′ positions. Therefore, as Whangbo et al. have already

Table 2. Calculated Transition Energies for a Series of $Ru(L)_2(NCS)_2$ Complexes, Where L Represents the 2,2′-Bipyridine-Derived Ligands Shown in Figure 9

ligand		ruthenium complex	
substituent	$E(\Pi^*_{bpy})$ (hartrees)	λ (MLCT) (nm)	Δ (cm^{-1})
H	−0.05014	425	27840
4,4′-COOH	−0.08637	454	25935
5,5′-COOH	−0.09250	503	23806
4,4′-PO_3H_2	−0.07456	437	27131
5,5′-PO_3H_2	−0.08004	466	25551
4,4′-COO^-	+0.15380		
4,4′-PO_3^{2-}	+0.36107		

suggested, it is expected that there will be a stronger inductive effect of the carboxylic group when bpy is substituted in 5,5′ positions.[32] In this sense, we observe that the energies of the lowest LUMO and MLCT transition are lower in this last case (Table 2).

When the bpy is functionalized by phosphonic acid groups, results similar to the those obtained with the carboxylic substituents are found. A decrease in the energies of the lowest LUMO of the dpbpy ligand and of the MLCT transition is also obtained. However, this decrease is lower than in the H_2dcb case, so this is an intermediate situation with respect to bpy and H_2dcb. This difference is due to the fact that the sp^3 hybridization in the phosphorus atom does not favor the interaction with the bpy π^* LUMO and, as a result, a weaker inductive effect occurs, as it also happens when there is a loss of coplanarity between the bpy and the carboxylic groups in the H_2dcb case (cf. Figure 9).

Furthermore, the protons in the anchoring group take electron density from this group, increasing the inductive effect of the substituent on the bpy ligand. Thus, deprotonation induces an excess of electron density on the anchoring group, and consequently, the mentioned attractive effect disappears while the charge excess is partially sent to the bipyridine ligand. Therefore, the energies of the lowest LUMO of the bipyridine ligand and of the MLCT transition increase (cf. Figure 9 and Table 2). This effect is more pronounced for the phosphonic acid compared to the carboxylic acid (Table 2), which is consistent with the largest increase of the electron density on the bipyridine due to the presence of the two negative charges of the phosphonate dianion (PO_3^{2-}) compared to only one on the carboxylate anion (CO_2^-). Furthermore, the destabilization induced upon deprotonation of the phosphonic acidic groups (PO_3H_2) shifts the energy level of the LUMO orbitals at energy higher than that of the unsubstituted bipyridine. In photovoltaic cells, the titanium(IV) ions bound to the dye sensitizers play a similar role as the protons in the anchoring group, increasing the inductive effect and shifting the MLCT transition to a less energetic region.

Unfortunately, this qualitative analysis only allows us to compare a series of compounds where a single factor is changed (nature of anchoring group, substitution position, or degree of protonation of the anchoring functions). Since

(32) Ohsawa, Y.; Whangbo, M. H.; Hanck, K. W.; DeArmond, M. K. *Inorg. Chem.* **1984**, *23*, 3426.

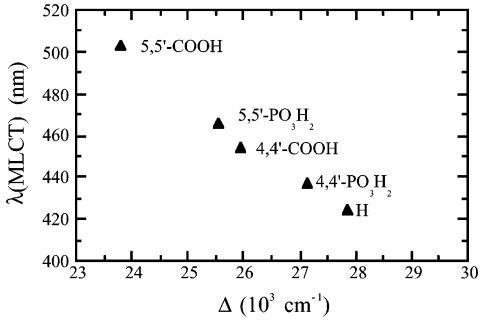

Figure 10. Correlation of the lowest energy MLCT transition with the energy gap (Δ) between the lowest Π^*_{bpy} LUMO and d_{Ru} HOMO involved in this transition.

the d_{Ru} HOMOs are not completely indifferent to the bipy substituents, the energy gap (Δ) between the lowest Π^*_{bpy} LUMO and the highest d_{Ru} orbital of the complexes involved in the MLCT transition must be considered to perform a global analysis of consequences accompanying these modifications. Although the energies of the LUMOs have no physical meaning, a perfect correlation is found between the energy of the MLCT transition and the Δ parameter (cf. Figure 10 and Table 2). The energy level of the MLCT transition can be qualitatively approximated with the above correlation with only an evaluation of the Δ parameter, which saves expensive TDDFT calculations.

The MO calculations have shown that the phosphonated bipyridines have a less stabilized π LUMO orbital with respect to carboxylated bipyridines. Electron-density delocalization on the anchoring group induces a stabilization of the lowest LUMO of the bipyridine ligand, thus decreasing the energy of the MLCT transition. Accordingly, it is important that the anchoring group interacts strongly with the Π^*_{bpy} orbitals of the bipyridine, as it is the case of the carboxylic group but not of the phosphonic acid substituent. The substituent position can intensify the mentioned effect. On the contrary, deprotonation of the anchoring group leads to a reorganization of the electron density that counterbalances the inductive effect and raises the energy of the Π^*_{bpy} LUMOs.

Conclusions

The preparation of the complexes *cis*-Ru(bipyridine bis phosphonic acid)X_2 with X = Cl, CN, or NCS (**5**−**10**) has been successfully achieved via the synthesis of the key intermediates **3** and **4**. These two compounds can represent useful synthons for the preparation of other ruthenium complexes containing two bipyridines functionalized with phosphonate groups. NMR spectroscopy demonstrates that the structures of the complexes correspond to the cis geometry and that the thiocyanato ligands are bound through the nitrogen atom. The spectroscopic and electrochemical characterizations of the new complexes show that they exhibit a blue-shifted electronic absorption spectrum and less anodic potentials of the $Ru^{III/II}$ couple with respect to the analogous complexes containing carboxylic acid groups. MO calculations allow the rationalization of these results, showing that the LUMO of the phosphonated bipyridine ligands is at higher energy. This is due to the lack of the mesomeric effect due to the sp^3-hybridized phosphorus atom. This effect is present with an sp^2 carbon atom and increases the resonance energy of the bipyridine substituted with carboxylic acid functions.

Calculations of electronic transitions show that the thiocyanato ligands are not simple spectator ligands, whose role is to enrich electron density on the ruthenium metal, raising the energy of the HOMO of the complex, but are also involved in a transitions from Π^*_{Ru-NCS} to Π^*_{bpy} orbitals that appear in the low-energy part of the absorption spectrum. This transition is of particular relevance since it extends the absorption in the red part of the visible spectrum.

The new ruthenium complexes have been studied as photosensitizers in regenerative solar cells. The photoaction spectra have shown that these complexes exhibit a lower overall efficiency with respect to the analogous species with carboxylated ligands, and this has been rationalized by the lower absorbance exibited in the red part of the visible spectrum. The fact that the RuL'_2X_2 sensitizers (complexes **6**, **8**, and **10**) show lower photoconversion efficiencies with respect to the corresponding RuL_2X_2 (complexes **5**, **7**, and **9**), despite the similarities of their redox and spectroscopic properties and the high electronic density in the 5,5′ position, is at present unclear. One possible explanation could be related to the orientation of the anchoring groups in 5,5′ positions, which can reduce the number of bonds between the sensitizer and the semiconductor surface. If this factor plays a role, it would be reflected by a lower coupling and rate of charge injection to the semiconductor. Ultrafast kinetic measurements will be carried out to clarify this point.

Acknowledgment. We thank the Ivory-Cost Ministry of Research and Education for the fellowship for Hervé Zabri and Dr. Mohammed Boujita from L.A.I.E.M. (Nantes University) for his kind assistance with the recording electrochemical data.

IC034403M